



ISSN: 2447-3359

REVISTA DE GEOCIÊNCIAS DO NORDESTE

*Northeast Geosciences Journal*

v. 9, nº 2 (2023)

<https://doi.org/10.21680/2447-3359.2023v9n2ID30719>



## Erosivity and erodibility mapping of the humid slope of the Massif and Uruburetama/CE surroundings as a subsidy for environmental planning

### *Mapeamento da erosividade e erodibilidade da vertente úmida do Maciço de Uruburetama/CE e entorno como subsídio ao planejamento ambiental*

Eduardo Viana Freires<sup>1</sup>, Cláudio Ângelo Silva Neto<sup>2</sup>, Cynthia Romariz Duarte<sup>3</sup>, César Ulisses Vieira Veríssimo<sup>4</sup>, Daniel Dantas Moreira Gomes<sup>5</sup>, Maykon Targino da Silva<sup>6</sup>, Débora Nogueira Lopes<sup>7</sup>

<sup>1</sup> Federal University of Ceará, Graduate Program in Geology, Fortaleza/CE, Brasil. Email: eduardovgeo@gmail.com

ORCID: <https://orcid.org/0000-0001-7010-5260>

<sup>2</sup> Federal University of Ceará, Graduate Program in Geology, Fortaleza/CE, Brasil. Email: claudioasn@gmail.com

ORCID: <https://orcid.org/0000-0002-6749-9438>

<sup>3</sup> Federal University of Ceará, Department of Geology, Fortaleza/CE, Brasil. Email: cynthia.duarte@ufc.br

ORCID: <https://orcid.org/0000-0002-0255-4045>

<sup>4</sup> Federal University of Ceará, Department of Geology, Fortaleza/CE, Brasil. Email: verissimo@ufc.br

ORCID: <https://orcid.org/0000-0002-5055-9617>

<sup>5</sup> University of Pernambuco, Department of Geography, Recife/PE, Brasil. Email: daniel.gomes@upe.br

ORCID: <https://orcid.org/0000-0001-6868-040X>

<sup>6</sup> Federal University of Ceará, Graduate Program in Geology, Fortaleza/CE, Brasil. Email: maykonts2011@gmail.com

ORCID: <https://orcid.org/0000-0002-9486-2714>

<sup>7</sup> Federal University of Goiás, Department of Geology, Goiânia/GO, Brasil. Email: deboranogueira@ufg.br

ORCID: <https://orcid.org/0000-0002-3329-0011>

**Abstract:** Erosive processes result from natural and human factors. Anthropogenic activities exacerbate soil loss due to inadequate management, compromising agricultural productivity and sustainability. This research aims to map the erosivity and erodibility of the Uruburetama/CE Massif's humid slope and surrounding area to support soil protection and management measures against water erosion. To generate the Erosivity Map, the IDW interpolator calculated erosivity based on rainfall records from 23 FUNCEME monitoring stations over ten years (2010-2019). The erosivity classes are associated with the behavior of local rainfall systems, which weaken as they move inland. As a result, we observed the occurrence of Moderate to Strong (92.66%) and Strong (7.34%) erosivity classes. We employed Ordinary Kriging for the soil erodibility analysis. We used the K-Factor derived from analyzing 92 soil samples (including granulometry, soil structure, and organic matter) and 92 undisturbed samples for permeability collected within the research area. The distribution and characteristics of local soils are the factors that establish the connection to the erodibility classes. The Planossolo Háplico Eutrófico and Neossolo Quartzarênico Órtico are associated with the Very Low class (8%). The Red-Yellow Argissolo and Neossolo Litólico are linked to the Low erosivity class (83%). On the other hand, the Moderate class (9%) is associated with Chromic Luvisol.

**Keywords:** Erosive processes; Handling; Anthropic activities.

**Resumo:** Os processos erosivos são gerados por causas naturais e humanas. As atividades antrópicas potencializam a perda de solos a partir de manejos inadequados e comprometem a produtividade agrícola e a sustentabilidade. Esta pesquisa objetiva realizar o mapeamento de erosividade e erodibilidade da vertente úmida do Maciço de Uruburetama/CE e entorno com o intuito de subsidiar medidas de proteção e manejo dos solos contra a erosão hídrica. O Mapa de erosividade foi obtido pelo interpolador IDW através do cálculo de erosividade realizado com base em registros pluviométricos de 23 estações de monitoramento da FUNCEME num intervalo de 10 anos (2010-2019). As classes de erosividade estão associadas a atuação de sistemas geradores de chuvas locais, que perdem força em direção ao continente. Assim, observou-se a ocorrência das classes de erosividade Moderada a Forte (92,66%) e Forte (7,34%). A erodibilidade dos solos foi processada por Krigagem Ordinária a partir do fator K obtido das análises de 92 amostras de solos deformadas (granulometria, estrutura do solo, matéria orgânica) e 92 indeformadas (permeabilidade) coletadas na área de pesquisa. As classes de erodibilidade estão associadas à distribuição e as características dos solos locais. A classe Muito Baixa (8%) está associada ao Planossolo Háplico Eutrófico e ao Neossolo Quartzarênico Órtico. A classe Baixa (83%) relaciona-se à ocorrência de Argissolo Vermelho-Amarelo e ao Neossolo Litólico, enquanto a classe Moderada (9%) associa-se ao Luvisolo Crômico.

**Palavras-chave:** Processos erosivos; Atividades antrópicas; Manejo.

Received: 31/10/2022; Accepted: 20/03/2023; Published: 24/07/2023.

## 1. Introduction

Soil is a country's most important natural resource because it derives the products to feed its population. In the intertropical regions, this importance is even more significant for two reasons: first, this zone is home to most of the developing countries, whose economy depends on the exploitation of their natural resources, especially agricultural ones; second, the processes that lead to the formation of soils can, in the intertropical zone, also lead to the formation of essential mineral resources. The soils of tropical regions are generally weathered, fragile, chemically depleted, and continuously evolving. In such a way, they exist in a situation of precarious equilibrium, in which the impacts caused by natural or anthropic causes can destabilize the system. Deforestation, land cultivation, use of agrochemicals, and mineral exploration are activities that, if not well conducted through techniques developed with a careful scientific basis, can lead to soil erosion and contamination (TOLEDO; OLIVE TREE; MELFI, 2003).

Human activities have caused widespread damage to soils and vegetation cover worldwide. However, it is more prominent in regions where disorderly land occupations occur or where the need for survival predominates over economic, social, and environmental factors (PALMIERI; LARACH, 2004).

According to Jorge and Guerra (2013, p.10), "[...] soils form, on average, at a rate of 1t/ha/year, and in Africa, Asia, and South America, losses reach 30t/ha/yr [...]"

Wind and water erosion usually causes soil erosion. In Brazil, due to its tropical location and high rainfall rates, water erosion prevails from the impact of raindrops and soil particle drag on land without vegetation cover (PRUSKI, 2009).

Although it occurs naturally, this geological process can be intensified and accelerated by anthropogenic activities, especially concerning changes in cover and intensive land use (NASCIMENTO; POMROME; SALES, 2018).

Among the main factors that condition erosion are rainfall erosivity, soil erodibility, relief characteristics, and vegetation cover (RANIERI *et al.*, 1998; SILVA; SCHULZ; CAMARGO, 2003)

Thus, there is a need to understand the erosive processes associated with the physical properties of the soil (erodibility) and the kinetic energy of rainfall (erosivity) to guide the occupation and use of the soil, respecting its natural vocation. Understanding these processes will allow planning that guarantees the rational use of the soil resource, enabling an adaptation between the potentialities of the land to the alternatives of use, conservation, and sustainable exploitation.

For Ross (2004), it is increasingly necessary to make anthropic insertions compatible with the potentialities of natural resources on the one hand and with the fragilities of natural environmental systems on the other.

In this sense, this research aims to map the erodibility and erosivity of the wet slope of the Uruburetama/CE Massif and its surroundings in order to identify the areas with the most significant susceptibility to water erosion so that it can subsidize the measures of protection and management of the soil against erosive processes.

## 2. Characterization of the study area.

The delimited area of this research (Figure 1) is located within the administrative limits of 9 municipalities (Irauçuba, Itapajé, Itapipoca, Pentecoste, Tejuçuoca, Trairi, Tururu, Umirim, and Uruburetama), which, according to the IBGE (2023), have in their entirety an estimated population for the year 2021 of approximately 383,621 inhabitants. This fact not only refers to the pressure exerted on the area but also reflects the difficulty of implementing environmental planning in the Massif.

"The mountain range of Uruburetama, positioned approximately 100 km west of Fortaleza, consists of a mountainous massif of circular shape, somewhat elongated in the direction E-W" (BRANDÃO; FREITAS, 2014). "It is intensely dissected in hills and ridges, with overimposed valleys, in the shape of a V, according to a parallel arrangement and oriented to NW-SE" (BRANDÃO, 2003). It is a residual massif with about 1000 km<sup>2</sup> of area, and its humid/subhumid portion corresponds to the northeastern slopes and the summit surface (plateau of the mountain). The Massif is strongly tectonized and intensely fractured, in which, in many cases, the drainage network adapts to these structures (SOUZA; OLIVEIRA, 2006).

Morphologically the studied area presents the following units: Tabuleiro Pré-litorâneo, Superfície Pediplanada (Depressão Sertaneja), Maciço Residual, Cristas Residuais e Inselbergs, Planícies Fluviais, and Planícies Alveolares.

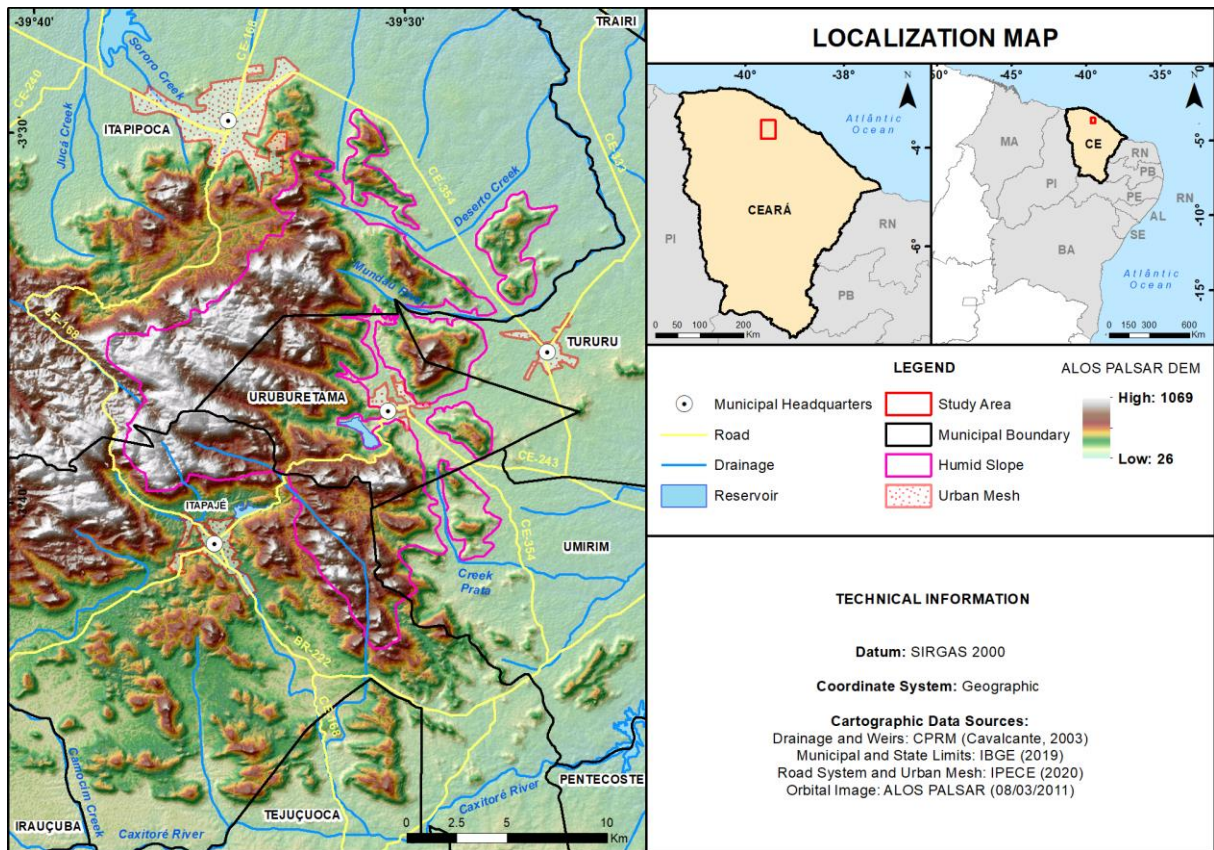


Figure 1 – Location map of the wet slope of the Uruburetama Massif.  
Source: The authors (2022).

The Uruburetama mountain range is inserted in an area of the Tropical Climate of the Equatorial Zone. According to Mendonça and Danni-Oliveira (2007), this type of climate is distributed throughout the North and Northeast regions and encompasses the entire state of Ceará.

"This climate is characterized by considerable rainfall and thermal variability. The temperature presents expressive spatial and temporal variability, even if the whole area is framed in the scope of the hot climates" (MENDONÇA; DANNI-OLIVEIRA, 2007, P.90).

The precipitation in the Serra de Uruburetama encompasses typical characteristics of a tropical regime, with the maximum in autumn and the minimum in winter. In the south/west sector, the average annual rainfall is 460 mm (municipal seat of Irauçuba). It usually presents three rainy months concentrated in late summer, and early autumn, between February, March, and April. The average annual rainfall in the north/east sector is 1,056 mm (headquarters of Uruburetama). It usually presents six to seven rainy months, concentrated in the year's first half (SILVA, 2007).

The following types of soils can be identified in the study area: Argissolo Vermelho – Amarelo Eutrófico, Neossolo Litólico Eutrófico, Neossolo Quartzarênico Órtico, Neossolos Regolítico Distrófico, Planossolo Háptico Eutrófico, and Luvissoilo Crômico Órtico (IBGE, 2017).

The soils are covered by the following plant formations: Vegetation complex of the coastal zone (Tabuleiro), dense scrub Caatinga, open shrubby Caatinga (Sertaneja depression); Tropical subdeciduous rainfall forest (dry forest) and tropical subperennial forest (humid forest) (IPECE, 2007).

## 2. Methodology

"The erosivity of rainfall represents a numerical index that expresses its capacity, expected in a given locality, to cause erosion in an unprotected area" (BERTONI; LOMBARDI NETO, 2012). In this research, erosivity was obtained from

rainfall records observed in the research area over ten years (2010 to 2019) through 23 rainfall stations (Table 1) of the Cearense Foundation of Meteorology and Water Resources (FUNCEME). The data were applied in Equation (1), proposed by Carvalho (1994), generating the value of erosivity in  $M.J.mm.ha^{-1}.h^{-1}.yr^{-1}$ .

Table 1 – Distribution of FUNCEME's Monitoring Stations by municipality and Erosivity obtained.

Municipality	Monitoring Station	Erosivity ( $M.J.mm.ha^{-1}.h^{-1}.yr^{-1}$ )
Amontada	Amontada	567.109
	Icarai de Amontada	1034.863
Apuiarés	Apuiarés	566.318
General Sampaio	General Sampaio	553.503
Irauçuba	Irauçuba	413.819
	Juá	424.011
Itapajé	Itapajé	592.038
	Santa Cruz	726.047
Itapipoca	Arapari	761.283
	Itapipoca	773.042
Miraíma	Miraíma	559.808
Paraipaba	Paraipaba	925.499
Pentecoste	Casa de Pedra	548.780
	Pentecoste	536.696
	Sebastiao de Abreu	551.542
São Gonçalo do Amarante	São Gonçalo	676.402
	Sede	815.620
	Siupe	987.263
São Luiz do Curu	São Luiz do Curu	602.088
Trairi	Fazenda Lages	777.646
	Trairi	881.699
Umirim	Umirim	605.908
Uruburetama	Uruburetama	667.216

$$Ecl = 6,866. (Pm^2 / P)^{0,85} \quad (1)$$

Where:  $Ecl$  = Monthly average of the erosion index;  $Pm$  = average monthly precipitation (mm);  $P$  = mean annual rainfall (mm).

Source: The authors (2022).

The values corresponding to the R-Factor were framed in the erosivity classes that Carvalho (1994) proposed, as seen in Table 2.

To evaluate the erosivity spatial distribution, we used the *Inverse Distance Weighting (IDW)* interpolation. According to Jakob and Young (2006), it is an interpolator that implements the assumption that things closer to each other are more similar than those farther apart. Thus, in order to infer a value for some unmeasured location, the IDW will use the values sampled around it, which will have a greater weight than the more distant values, or rather, each point will maintain an influence on the new point, which decreases as the distance increases, hence its name.

Table 2 – Erosivity rates of the mean annual classes.

Erosivity Classes	R-value
Weak	$R < 250$
Moderate	$250 < R < 500$
Moderate to Strong	$500 < R < 750$
Strong	$750 < R < 1000$
Very strong	$R > 1000$

Source: Carvalho (1994).

## 2.2 Soil erodibility determination (K-Factor)

Erodibility, or K-Factor, represents the susceptibility or predisposition of soil to erosive processes (WISCHMEIER; SMITH, 1978). The lower the stability of soil aggregates and water infiltration capacity, the greater susceptibility to erosive processes. Soils rich in silt and sand and with cementing material (organic matter and iron and aluminum oxides) are very prone to erosive processes due to the small resistance they offer to the detachment of particles during precipitation (PRUSKI, 2009).

The erodibility of soils was indirectly determined through the Nomograph (Figure 2) proposed by Wischmeier, Johnson, and Cross (1971).

For this, we collected 184 soil samples, of which 92 were deformed, and 92 were undeformed (Figure 3), in six field incursions (17 days). The deformed samples were submitted to laboratory tests to determine the granulometry, organic matter content, and soil structure. At the same time, we used the undisturbed samples to determine the permeability of the soil.

The analysis in the nomograph is based on the integration of the parameters of granulometry, organic matter content, soil structure, and permeability obtained through laboratory tests, of the samples of deformed and undeformed soils, according to ABNT soils standards (Figure 4).

To apply the values obtained in the analyses and to obtain the erodibility factor with greater precision, Equation (2) was used, which represents an algebraic approximation of the Nomograph (ARS/USDA, 1997).

$$K = \left\{ \frac{[2,1(10^{-4})(12 - MO)M^{1,14} + 3,25(s - 2) + 2,5(p - 3)]}{100} \right\} 0,1318 \quad (2)$$

Where:  $K$  = Erodibility ( $t.ha.h (ha.MJ.mm)^{-1}$ );  $OM$  = Organic matter content, %;  $M$  = Parameter representing the texture of the soil;  $s$  = Soil structure class;  $p$  = permeability.

The  $M$  parameter is calculated from Equation (3):

$$M = (\% \text{ silt} + \% \text{ very fine sand}).(100 - \% \text{ clay}) \quad (3)$$

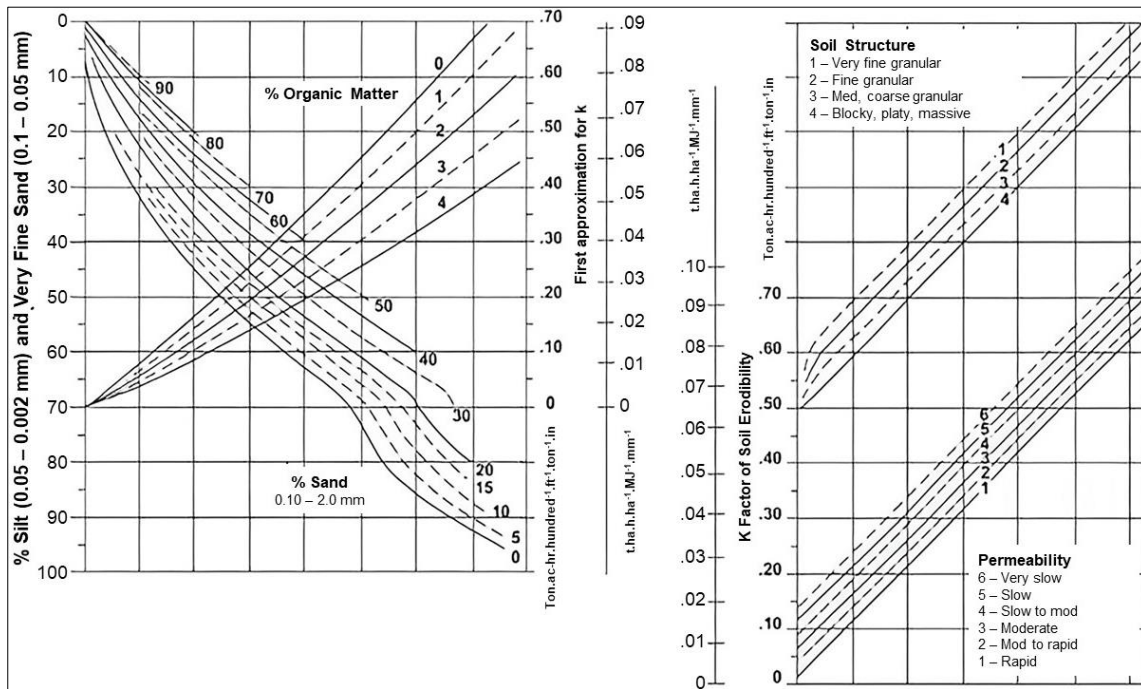


Figure 2 – Nomograph to determine soil erodibility. Source: Wischmeier, Johnson, and Cross (1971).  
Source: The authors (2022).

For the granulometric analysis, the 92 deformed soil samples collected were submitted to the procedures established by NBR 7181 (ABNT, 1984), which prescribes the method for granulometric analysis of soils, performed by sieving or by combining sedimentation and sieving. This test determines the soil particle size distribution, *i.e.*, the percentage by weight that each specified grain size range represents in the total dry mass used for the test.

To perform the test, NBR 5734 (ABNT, 1989), which specifies the sieves for testing, and NBR 6457 (ABNT, 1986), which deals with the preparation of soil samples for compaction tests and characterization tests, were used in complementary way.

The structure reflects the resistance of the soil to erosion through the physicochemical properties of the clay, which makes the aggregates remain stable in the presence of water and biological properties due to the presence of humified organic matter. The greater the stability of the aggregates in water, the greater the permeability of the soil and the lower the disaggregation, implying the lower surface runoff and drag of the particles individualized by the water (CORRECHEL, 2003).

Table 3 presents the classes of these structures and their corresponding categories. The ‘s’ values for soils of very fine, fine granular, medium to coarse granular structure and in block, lamina, or massive are 1, 2, 3, and 4 (WISCHMEIER; JOHNSON; CROSS, 1971).

The category values of the soil structure of the research area were defined from the results obtained through the granulometric analysis of the samples, where the percentage of each size of sediments can be verified.

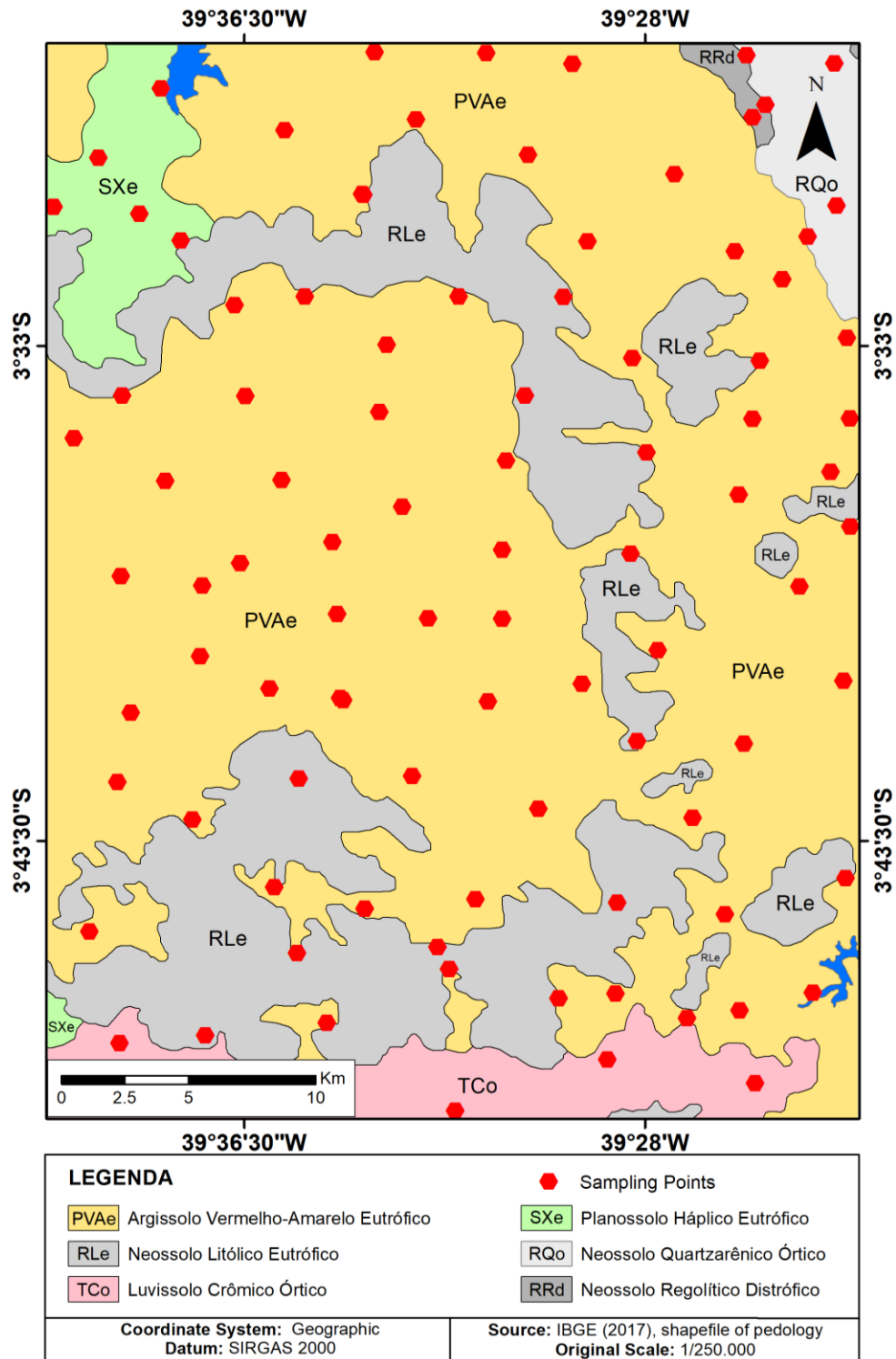


Figure 3 – Distribution of collected samples of soil obtained in the research area.  
Source: The authors (2022).

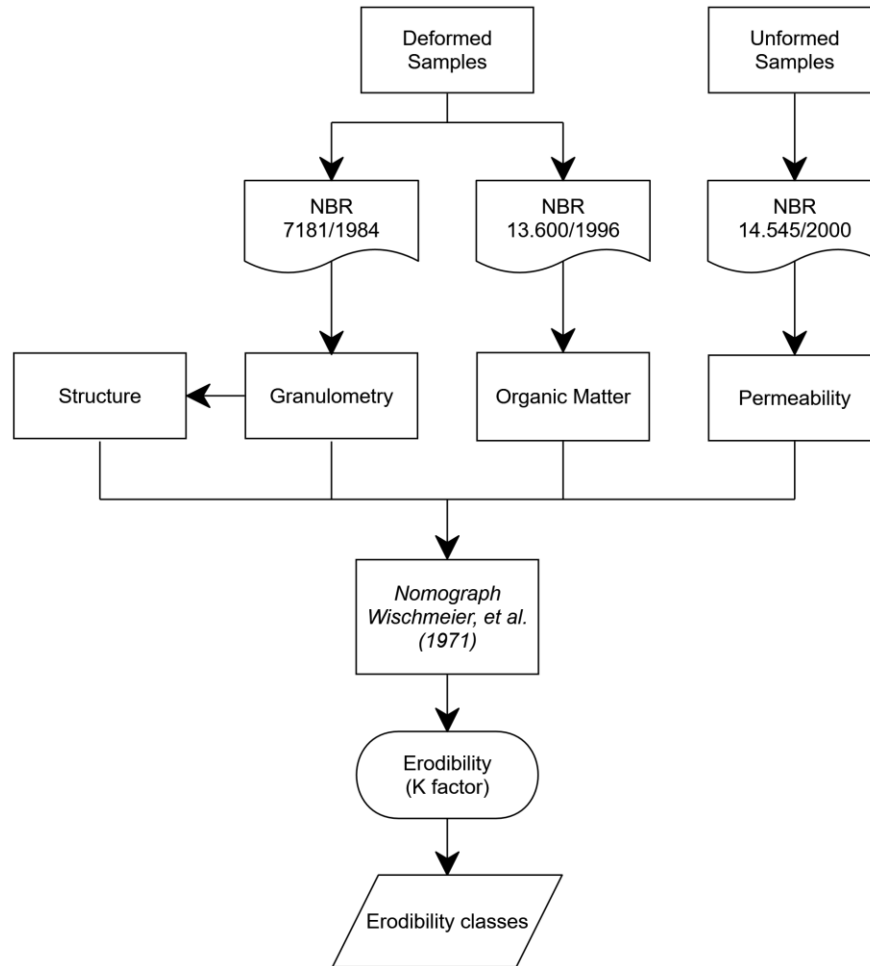


Figure 4 – Flowchart for determination of erodibility.  
Source: The authors (2022).

Table 3 – Classes and categories of soil structure.

Structure Category	Classification
1	Very fine granular (> 50% thin)
2	Fine granular (> 50% sand)
3	Medium to coarse granular (> 50% coarse sand)
4	Blocky, platy, massive (> 50% gravel)

Source: Adapted from Wischmeier, Johnson, and Cross (1971).

0.5 kg of the deformed sample obtained in the field was used to analyze the organic matter. This test was performed according to NBR 13600 (ABNT, 1996), which describes the procedures for determining the organic matter content by burning at 440°C.

Equation (4) was used in the calculations to determine the organic matter content:

$$MO = \left(1 - \frac{B}{A}\right) \times 100 \quad (4)$$

Where:  $MO$  = organic matter content in %;  $A$  = mass of the sample dried in an oven at a temperature of 105 °C to 110 °C in g;  $B$  = mass of the sample burned in muffle at a temperature of  $(440 \pm 5)$  °C in g.

Soil permeability is essential for erodibility analysis because the higher the infiltration, the lower the runoff and, consequently, the lower the erosive potential. The permeability test determines the permeability coefficient with water percolating through the soil in a laminar runoff. The permeability tests of the 92 samples of undisturbed soils were performed according to NBR 13292 (ABNT, 1995), a norm that governs the determination of the permeability coefficient of granular soils at constant load, and NBR 14545 (ABNT, 2000), which deals with the determination of the permeability coefficient of clay soils at variable load.

The calculation of permeability by constant charge was based on Equation (5):

$$K = \frac{Q \cdot L}{A \cdot H \cdot t} \quad (cm/s) \quad (5)$$

Where:  $K$  = Permeability coefficient per constant charge (cm/s);  $Q$  = Volume of water measured in the beaker (cm<sup>3</sup>);  $L$  = Height of the specimen (cm);  $A$  = Area of the specimen (cm<sup>2</sup>);  $H$  = Hydraulic load (cm);  $t$  = Elapsed time of the test (s).

The calculation of the permeability coefficient by variable load was given by Equation (6):

$$K_{20} = 2.3 \times \frac{aL}{At} \times \log \frac{h_o}{h_f} \times Fc \quad (6)$$

Where:  $K_{20}$  = Permeability Coefficient by variable load (cm/s);  $a$  = cross-sectional area of the burette (cm<sup>2</sup>);  $L$  = Diameter of the specimen (cm);  $A$  = Cross-sectional area of the specimen (cm<sup>2</sup>);  $t$  = Time elapsed from the test (s);  $H_o$  = Initial height of the water level (cm);  $H_f$  = Final height of the water level (cm).

Table 4 presents the values and permeability classes. The p values for soils with fast, moderate to fast, moderate, slow to moderate, slow, and very slow permeability are 1, 2, 3, 4, 5, and 6, respectively (WISCHMEIER; JOHNSON; CROSS, 1971).

Table 4 – Classification of soil permeability values with variable and constant load.

Permeability code	Classification	Permeability intervals (cm/s)
6	Very slow	$< 2,8 \times 10^{-5}$
5	Slow	$2,8 \times 10^{-5} - 5,6 \times 10^{-5}$
4	Slow to moderate	$5,6 \times 10^{-5} - 1,46 \times 10^{-4}$
3	Moderate	$1,46 \times 10^{-4} - 5,6 \times 10^{-4}$
2	Moderate to rapid	$5,6 \times 10^{-4} - 1,7 \times 10^{-3}$
1	Rapid	$> 1,7 \times 10^{-3}$

Fonte: Adapted from Wischmeier, Johnson, and Cross (1971).

### 2.2.1 Spatialization of erodibility (K-Factor) by Ordinary Kriging

With the K-Factor obtained from all sampling points according to the proposed methodology, each value was framed within the erodibility classes proposed by McKenzie, Coughbon, and Cresswell (2002), observed in Table 5.

For spatialization of the K-Factor and later of the erodibility classes, an interpolation was performed by the ordinary *Kriging* method.

*Kriging* is a geostatistical process of estimating the values of variables distributed in space or time based on adjacent values when considered interdependent by variogram analysis. The fundamental difference to estimates by weighted

averages or moving averages is that only Kriging presents unbiased estimates and the minimum variance associated with the estimated value (YAMAMOTO; LANDIM, 2013).

Table 5 – Classification of erodibility.

Intensity of erodibility	K-Factor range (t.ha.h (ha.MJ.mm) <sup>-1</sup> )
Very low	< 0,01
Low	0,01 – 0,02
Moderate	0,02 – 0,04
Loud	0,04 – 0,06
Very High	> 0,06

Source: McKenzie, Coughbon, and Cresswell (2002).

According to Yamamoto and Landim (*op. cit.*), ordinary *Kriging* is a local method of estimation in which an unsampled point results from the linear combination of values found in the nearby neighborhood. The estimator of ordinary Kriging is based on the weighted average formula, where the weights depend on the structural information provided by the variogram. The value of the variable of interest at an unsampled point ( $x_0$ ) is calculated as a linear combination of the neighboring data points ( $Z(x_i), i=1, n$ ), according to Equation (7):

$$Z_{KO}^*(x_0) = \sum_{i=1}^n \lambda_i Z(x_i) \tag{7}$$

where  $Z_{KO}^*$  = estimator of ordinary Kriging,  $x_0$  = the unsampled site,  $n$  = values obtained at adjacent points,  $\lambda_i$  = weights assigned to each known value,  $Z(x_i)$  = a value estimated by *Kriging*.

The GeoMS Software (CMRP-CERENA, 2001) was used to construct and model the variogram, where the parameters for such procedures were defined.

As shown in Figure 5, the main direction (45°) and the orthogonal or secondary direction (- 45°) were identified from the distribution and variance of the samples. The azimuths transverse to these axes were defined based on these directions, *i.e.*, 0° and 90°. Under the possibility of the samples presenting a similar behavior in all directions, an omnidirectional azimuth was defined, represented by 1°.

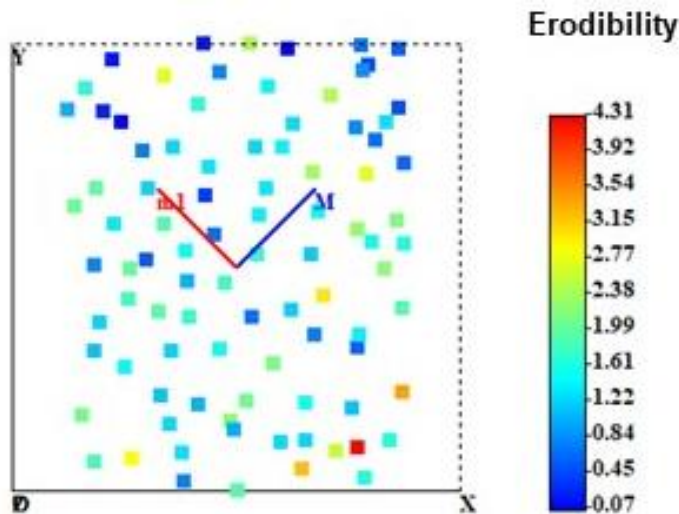


Figure 5 – Distribution of samples with main (M) and secondary (m1) directions. Source: The authors (2022).

From the azimuths identified, the values of the parameters for the construction of the variograms were defined (Table 6).

The variograms were modulated or adjusted in the next step to infer the distance or representative amplitude for the area and pairs of points according to the established directions. With the adjustment, it was also sought to reduce the nugget effect.

Table 6 – Parameters used for the construction of the variogram.

Azimuth	Parameters	Values	Azimuth	Parameters	Values
45°, -45°, 0°, and 90°	Tolerance	12	Omnidirectional 1°	Tolerance	180
	Lag Distance	3500		Lag Distance	3500
	Cut Distance	100000		Cut Distance	100000

Source: The authors (2022).

The nugget effect measures the variability corresponding to a small scale not covered by the sampling mesh and the variability to the scale of the sample induced by non-systematic sampling and monitoring errors that add to the structure of the phenomenon a random noise (SOARES, 2006).

All variograms were modulated using a spherical model. According to Soares (2006), the spherical model is a function of two parameters: a level C, the upper limit to which the values of the variogram tend with the increase of the values of h, and the amplitude h=a, the distance from which the values of  $\gamma(h)$  stop growing and are equal to a level that is usually coincident with the variance of Z(x). The amplitude measures the distance from which the Z(x) values cease to be correlated.

After adjusting all variograms, the one with the highest amplitude was selected, the variogram representative of the 45° direction and the orthogonal variogram in this direction, in this case – 45°, as seen in Figure 6.

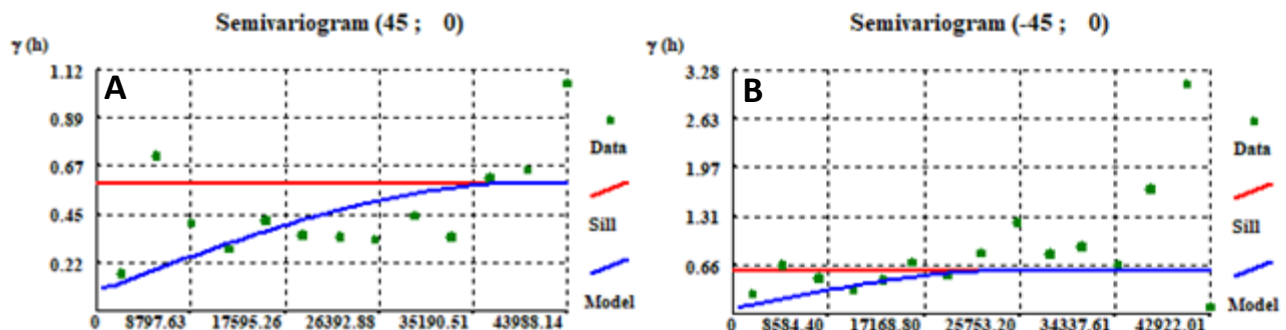


Figure 6 – (A) Variogram with direction 45°; (B) Variogram with direction – 45°.

Source: The authors (2022).

Based on the construction and modulation parameters of the variogram with a 45° direction, the sampling data (K-Factor) was krigged in the ArcGIS® 10.5 software (ESRI, 2017). These parameters can be seen in Table 7.

A distribution map of the interpolated samples in 10 classes was generated from the kriging process. Subsequently, the classes were redefined according to the erodibility intervals of Mackenzie *et al.* (2002). This resulted in the erodibility map with three classes (Very Low, Low, and Moderate).

Table 7 – Parameters used in ordinary Kriging.

<b>Direction main</b>	<b>45°</b>
<b>Semivariogram model</b>	Spherical
<b>Lag size</b>	3500
<b>Number of lags</b>	12
<b>Major range</b>	40469.089
<b>Minor range</b>	25753.205
<b>Partial Sill</b>	0.5
<b>Nugget</b>	0.092
<b>Maximum Neighbors</b>	15
<b>Minimum Neighbors</b>	5

Source: The authors (2022).

### 3. Results and discussion

#### 3.1 Erosivity map

Figure 7 shows the distribution of erosivity in a regional context obtained from the IDW interpolator. It is possible to observe that the highest records of erosivity occur in the coastal municipalities due to the higher rainfall rates, such as São Gonçalo do Amarante, Paraipaba, Trairi, and Amontada. The volume of rainfall tends to decrease towards the continent's interior as rain-generating systems' performance decreases. On the other hand, the layout of the Uruburetama Massif favors the occurrence of orographic rainfall, which implies higher rainfall averages in the north/east sector and consequently higher erosivity rates in the windward portion of the mountain, as in sectors of the municipalities of Itapipoca and Uruburetama. On the other hand, the municipalities located to the leeward of the Massif, such as Irauçuba and Itapajé, have lower rainfall averages, which implies lower erosivity rates.

This trend is corroborated by Ribeiro Filho *et al.* (2017), which evidenced the rainfall variability in the State of Ceará for 34 years by spatializing the rainfall coefficient through the *kriging* method and finding values ranging from 1670 mm on the coast to 449 mm in the sertão region.

Figure 8 shows the distribution of erosivity classes in regional and local contexts by applying Carvalho classes (1994) and interpolating by IDW. As can be seen, the classes of Strong and Very Strong Erosivity are distributed mainly in the northern and northeastern portions, where the highest rainfall rates are associated with proximity to the coast, an area marked by the influence of smaller-scale precipitation generating systems, such as the lines of instability formed along the coast and sea and land breezes.

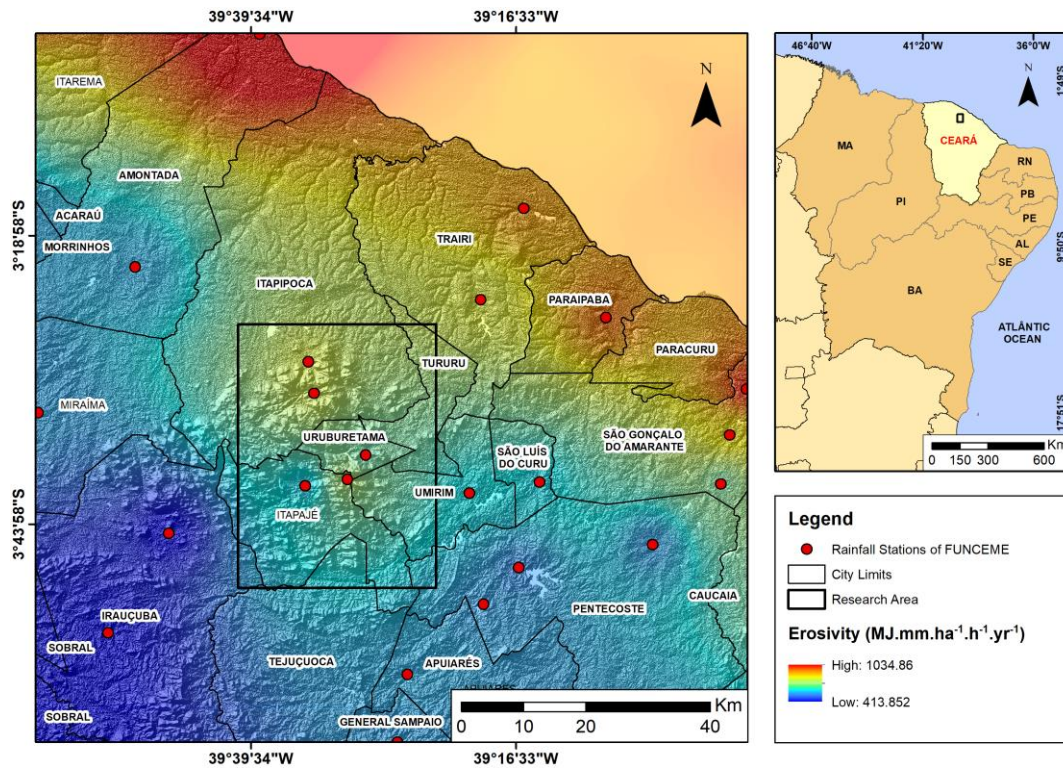


Figure 7 – Erosivity in the regional context and the area of study.  
Source: The authors (2022).

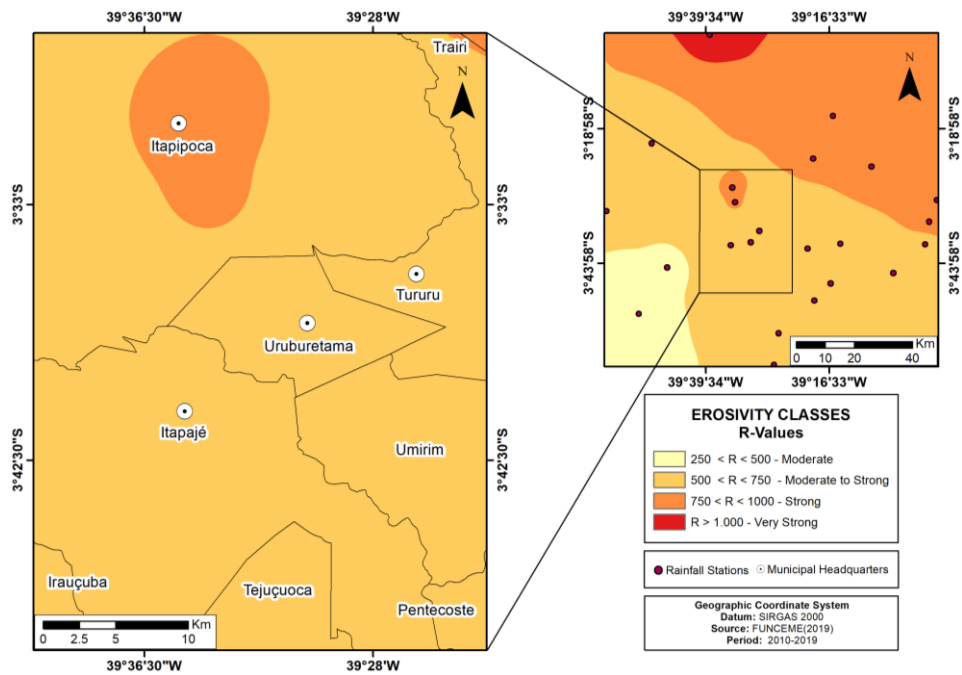


Figure 8 – Distribution of erosion classes in the regional and study areas.  
Source: The authors (2022).

Within the limits of the research area, only two classes of erosivity occur: Moderate to Strong, in almost its entirety, which represents 92.66%; and Strong Erosivity, restricted to portions of the municipalities of Itapipoca and Trairi, which totals 7.34%, whose rainfall seasons exceeded  $761 \text{ MJ.mm.ha}^{-1}.\text{h}^{-1}.\text{yr}^{-1}$ .

Due to the large extension of the Moderate to Strong erosivity area, it was impossible to associate the indices obtained with the soil and vegetation cover classes. This fact is due to the normalization of the class interval for different areas of soil patches and vegetation cover coverage.

Notably, the spatialization of these indices does not necessarily mean that the greater the erosivity of rainfall, the greater the soil loss due to erosion. This loss is also closely associated with management, soil type, and agricultural practices (SANTA'ANNA NETO, 1995).

Studying rainfall records in broader historical series (at least 20 years) is understood to be essential, as it ensures greater assertiveness in the analysis of erosivity. We considered a 10-year interval for the present study since these data were more regular. We chose a smaller historical series due to some stations' absence or incompleteness of rainfall records in specific months or years.

### 3.2 Erodibility map

Figure 9 shows the spatialization of soil erodibility in the wet slope of the Uruburetama Massif and its surroundings, generated from the data of granulometry, soil structure, organic matter, and permeability obtained from the 184 soil samples collected in the research area.

As can be seen, according to the classification of McKenzie, Coughbon, and Cresswell (2002), three classes of erodibility were found: Very Low Erodibility, Low Erodibility, and Moderate Erodibility.

The Very Low erodibility class represents 8% of the mapped area. It occurs in restricted sectors of the northern portion of the research area. We mainly observe these sectors in soils that have high percentages of sand in their composition, such as the Planossolo Háplico Eutrófico in the northwest and the Neossolo Quartzarênico Órtico in the northeast. These soils, because they present high permeability, favor the infiltration of rainwater, thus reducing the capacity of laminar erosion.

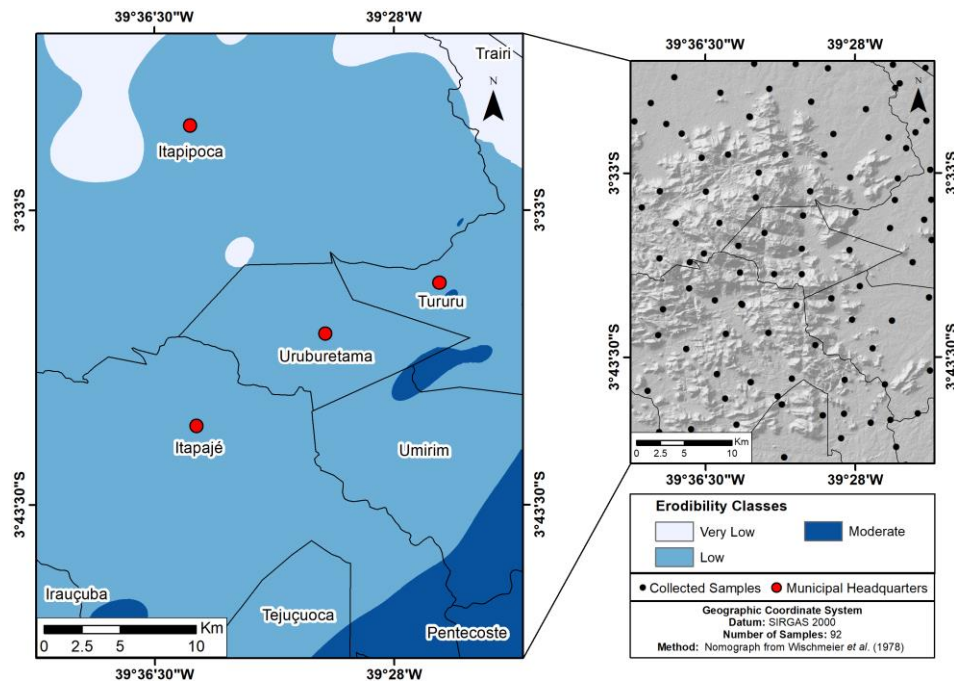


Figure 9 – Distribution of collection points and map of soil erodibility of the wet slope of the Uruburetama Massif and its surroundings.

Source: The authors (2022).

The Low Erodibility class covers 83% of the research area. It corresponds mainly to the occurrence of Argissolo Vermelho-Amarelo and Neossolo Litólico. The first is characterized by higher clay contents, reducing soil permeability and favoring runoff. On the other hand, the higher content of organic matter favors stability and infiltration. With excellent dispersion on the slopes and plateau of the Massif of Uruburetama, its stability depends on the slope percentage, the protection of the vegetation cover, and the type of management to which it is subjected.

Corn and bananas are the most widespread crops in the Uruburetama Massif. The degradation of these types of soils is directly associated with agricultural activity.

In the humid portion of the Uruburetama Massif, where the Red-Yellow Argissolos predominate, banana farming stands out (Figure 10). This culture is entirely inadequate to the environmental characteristics of the area. Placing natural vegetation with banana trees exposes large soil tracts to erosive agents. Associated with this is the fact that this plant has shallow roots that do not guarantee the stability of the soils and, when grown in steep areas, with significant rainfall or with an inadequate irrigation system, tend to trigger mass movements, which can be observed quite often in the humid slope of the Massif (FREIRES *et al.*, 2021).



Figure 10 – Banana cultivation in Red-Yellow Argisols on slopes in the municipality of Uruburetama/CE.  
Source: The authors (2019)

The Neossolo Litólico, in turn, being a shallow and stony soil, presents very slow permeability, which favors surface runoff. Cultivating temporary crops, such as corn, without applying appropriate techniques potentiates the erosive processes (Figure 11). It is common in the Massif the so-called downhill cultivation, in which planting is carried out in the sense of the flow, potentiating the floods and intensifying the erosive processes and the degradation of the soils. Added to this is the practice of burning, which precedes sowing and contributes to reducing soil fertility over the years. This type of cultivation results in the gradual loss of soil productivity until its complete degradation from the formation of ravines, which can evolve into gullies.



Figure 11 – Corn crops in Neossolo Litólico, in the downhill system, on slopes in the municipality of Itapajé/CE.  
Source: The Authors (2018).

In sectors to the south of the research area, marked by the occurrence of the Chromic Luvisol, which borders the Caxitoré River, and also in the surroundings of the Caxitoré Dam, the Moderate Erodibility class can be observed, which corresponds to 9% of the study area. The Luvisolo Crômico is characterized by high clay content and shallowness, often stony (EMBRAPA. 2009). This condition favors agricultural activity (figure 11); however, the prolonged use, without good management practices, makes the soil more erodible as the loss of organic matter, responsible for increasing the resistance of aggregates, occurs. In addition, there is a more significant contribution of fine sediments and organic matter in the surrounding area, especially in the floodplains, the Caxitoré River, and the reservoir. The occurrence of droughts in recent years has exposed these areas for an extended period to agricultural intervention, favoring the reduction of organic matter and, in turn, the resistance of the soil to laminar erosion. Consequently, these sectors show more potential for laminar erosion than the others mentioned.



Figure 11 – Cotton and grass crops on the banks of the dry bed of the Caxitoré River.  
Source: The authors (2017).

It is necessary to carry out complementary studies involving other variables, such as the one proposed by Salomão (2015) and applied by Silva and Mendes (2019), in the upper course of the Banabuiú River in the State of Ceará, which integrated erodibility data with a slope of the terrain and elaborated the Map of Susceptibility to Laminar Erosion. As well as studies that make estimates of soil loss from the *Universal Soil Loss Equation* (USLE), proposed by Wischmeier and

Smith (1978), and that integrate data with a higher degree of complexity, such as erosivity, erodibility, length, and slope of the slope, land use and management and conservation practices. Like what was done by Barbosa *et al.* (2015), who applied this methodology in the municipality of Paraiso da Águas, in Mato Grosso do Sul, from free and open *source software*.

#### 4. Final considerations

The erosivity distribution map obtained from the rainfall records of the 23 FUNCEME monitoring stations shows that the classes decrease in intensity towards the interior. This picture is related to the decay of the volume of rainfall that occurs towards the continent due to the reduction of the performance of the systems that generate rains of a smaller scale and present more incredible energy on the coast, such as sea and land breezes. As a result of this fact, only two classes of erosivity are observed in the research area: Moderate to Strong, which represents 92.66% of the area, and Strong Erosivity, which totals 7.34%. It is essential to understand that erosivity is a variable that expresses the ability of rain to cause erosion in unprotected soils. Its influence is more significant in deforested sectors, abandoned by itinerant agriculture, and temporary crop planting areas, which expose the soils for months. On the other hand, its performance is limited in areas with vegetation cover, especially in sectors covered by primary vegetation.

Regarding the distribution of the erodibility classes obtained from the 184 soil samples obtained in the field, it was observed that 8% of the mapped area corresponds to the Very Low Erodibility class. Its occurrence is associated with the Planossolo Háplico Eutrófico and the Neossolo Quartzarênico Órtico. The Low Erodibility class represents 83% of the area. It is related to the occurrence of Red-Yellow Argissolo and Neossolo Litólico. The Moderate Erodibility class is distributed over 9% of the research area. It is mainly associated with the Luvisolo Crômico, which borders the Caxitoré River and the floodplain area around the Caxitoré Dam. The erodibility classes indicate the susceptibility of the soils to erosive processes. However, it is necessary to analyze other variables together, such as the conservation status of the vegetation cover, rainfall indexes, topographic gradient, relief arrangement, and soil management.

Recognizing the susceptibility of soils to erosive processes is paramount for mitigating measures to be adopted to ensure agricultural sustainability. The erodibility and erosivity maps indicate the areas with the lowest and highest potential for erosive processes, considering soil properties and rainfall energy, respectively. This information is of great relevance, as it allows the establishment of preventive measures to reduce soil loss, which in most cases are derived from unplanned interventions and do not take into account factors such as type of soil, crop adopted, planting systematics, the slope of the land, the volume of rainfall and irrigation system employed.

#### Acknowledgments

The authors thank the Fundação Cearense de Apoio ao Desenvolvimento Científico e Tecnológico (FUNCAP) and the Coordenação de Aperfeiçoamento de Pessoal de Nível Superior (CAPES) for the financial support granted; and to the Graduate Program in Geology of UFC for encouraging this research.

#### References

- ABNT, Associação Brasileira de Normas Técnicas. *NBR 14545: Determinação do coeficiente de permeabilidade de solos argilosos a carga variável*. Rio de Janeiro, julho de 2000.
- ABNT, Associação Brasileira de Normas Técnicas. *NBR 13292: Determinação do coeficiente de permeabilidade de solos granulares a carga constante*. Rio de Janeiro, abril de 1995.
- ABNT, Associação Brasileira de Normas Técnicas. *NBR 13600: Determinação do teor de matéria orgânica por queima a 440°C*. Rio de Janeiro, maio de 1996.
- ABNT, Associação Brasileira de Normas Técnicas. *NBR 5734: Peneiras para ensaios com telas de tecido de metálico*. Rio de Janeiro, dezembro de 1989.
- ABNT, Associação Brasileira de Normas Técnicas. *NBR 6457: Preparação para ensaios de compactação e ensaios de caracterização*. Rio de Janeiro, agosto de 1986.
- ABNT, Associação Brasileira de Normas Técnicas. *NBR 7181: Solos - análise granulométrica.*, dezembro de 1984,

ARS-USDA, Agricultural Research Service. *Predicting soil*, 1994.

Barbosa, A. F.; Oliveira, E. F.; Mioto, C. L.; Paranhos Filho, A. C. Aplicação da Equação Universal de Perda do Solo (USLE) em Softwares Livres e Gratuitos. *Anuário do Instituto de Geociências*. v.38, n.1, 170-179, 2015.

Bertoni, J.; Lombardi Neto, F. *Conservação do solo*. 8ª ed. São Paulo: Ícone, 2012. 355p.

Brandão, R.L. Zoneamento Geoambiental da região de Irauçuba/CE. Texto explicativo. Carta Geoambiental. Fortaleza: CPRM, 2003. 67 p.

Brandão, R.L.; Freitas, L.C.B. *Geodiversidade do estado do Ceará*. Fortaleza: CPRM, 2014. 214 p.

Carvalho, N. O. *Hidrossedimentologia prática*. Rio de Janeiro: CPRM, 1994. 372p.

CMRP-CERENA, Centro de Recursos Naturais e Ambiente. *Geostatistical Modeling Software (GeoMS version 2001)*, Lisboa, Portugal.

CAVALCANTE, J. C.; VASCONCELOS, A. M.; MEDEIROS M. F.; PAIVA I. G. *Mapa Geológico do Estado do Ceará*. 1ª edição. Fortaleza: CPRM, 2003. Escala 1:500.000.

CORRECHEL, V. *Avaliação de índices de erodibilidade do solo através da técnica da análise da redistribuição do "Fallout" do <sup>137</sup>Cs*. 2003. Piracicaba, 2003. 79f. Tese. (Doutorado em ciências). Centro de Energia Nuclear na Agricultura, Universidade de São Paulo, Piracicaba-SP, 2003.

EMBRAPA, Empresa Brasileira de Pesquisa Agropecuária. *Sistema brasileiro de classificação de solos*. Rio de Janeiro: EMBRAPA-SPI, 2009. 367 p.

ESRI – Environmental Systems Research Institute. *Software ArcGIS Desktop (version 10.5)*. Redlands, Estados Unidos, 2017.

Freires, E. V.; Silva Neto, C. A.; Duarte, C. R.; Verissimo, C. U. V.; Gomes, D. D. M.; Maia, A. O. Diagnóstico da degradação ambiental na Vertente Úmida do Maciço de Uruburetama/CE e seu entorno. *Ciência e Natura*, v. 43, e18, 1-55, 2021.

IBGE, Instituto Brasileiro de Geografia e Estatística. *Portal das cidades: panorama/ população*. Brasília: Ministério do Planejamento, Orçamento e Gestão. Disponível em: <https://cidades.ibge.gov.br>. Acesso em: 15/09/2023.

IBGE, Instituto Brasileiro de Geografia e Estatística. *Mapa temático de Pedologia em escala de 1:250.000*. Brasília: Ministério do Planejamento, Orçamento e Gestão. Disponível em: [ftp://geoftp.ibge.gov.br/informacoes\\_ambientais/pedologia/vetores/escala\\_250\\_mil/recorte\\_milionesimo/](ftp://geoftp.ibge.gov.br/informacoes_ambientais/pedologia/vetores/escala_250_mil/recorte_milionesimo/). Acesso em: 10/01/2017.

IBGE, Instituto Brasileiro de Geografia e Estatística. *Malhas territoriais: vetores de municípios do Ceará e de Unidades Federativas do Brasil em escala de 1:250.000*. Brasília: Ministério do Planejamento, Orçamento e Gestão. Disponível em: <https://www.ibge.gov.br/geociencias/organizacao-do-territorio/malhas-territoriais/15774-malhas.html?=&t=acesso-ao-produto>. Acesso em: 05/12/2019.

IPECE, Instituto de Pesquisa e Estratégia Econômica do Ceará. *Ceará em Mapas: arquivos georreferenciados. Dados vetoriais: sistema viário e mancha urbana*. Disponível em: <http://mapas.ipece.ce.gov.br/i3geo/ogc/index.php>. Acesso em: 10/05/2020.

IPECE. Instituto de Pesquisa e Estratégia Econômica do Ceará. *Mapa das unidades fitoecológicas do Estado do Ceará em Escala 1:250.000*. Fortaleza: IPECE, 2007. Disponível em: [http://www2.ipece.ce.gov.br/atlas/capitulo1/12/images3x/Unidades\\_Fitoecologicas.jpg](http://www2.ipece.ce.gov.br/atlas/capitulo1/12/images3x/Unidades_Fitoecologicas.jpg). Acesso em: 26/03/2016.

JAKOB, A. A. E.; YOUNG, A. F. O uso dos métodos de interpolação espacial de dados nas análises sociodemográficas. In: XV Encontro Nacional de Estudos Populacionais, 15., 2006, Caxambu. *Anais do XV Encontro Nacional de Estudos*

*Populacionais*. Caxambu-MG: ABEP, 2006, p.1-22. Disponível em: <http://www.nepo.unicamp.br/vulnerabilidade/admin/uploads/producoes/MétodosInterpolação> . Acesso em: 23/03/2020.

- JORGE, M. C. O.; GUERRA, A. J. T. Erosão dos solos e movimentos de massa: recuperação de áreas degradadas com técnicas de bioengenharia e prevenção de acidentes. In: GUERRA, A. J. T.; JORGE, M. C. O (Org.). *Processos erosivos e recuperação de áreas degradadas*. São Paulo: Oficina de Textos, 2013. p. 7-30.
- Mckenzie, N. J.; Coughbon, K. J.; Cresswell, H. P. *Soil Physical Measurements and Interpretation for Land Evaluation*. Melbourne: CSIRO Publishing, 2002. 392p.
- Mendonça, F.; Danni-Oliveira, I. M. *Climatologia: noções básicas e climas do Brasil*. São Paulo: Oficina de Textos, 2007. 206p.
- Nascimento, D. T. F.; Romão, P. A.; Sales, M. M. Erosividade e erodibilidade ao longo de dutovia cortando os estados de Minas Gerais e Goiás – Brasil. *Atêlie Geográfico*, v. 12, n. 1, 97-117, 2018.
- PALMIERI, F.; LARACH, J. O. I. Pedologia e geomorfologia. In: GUERRA, A.J.T.; CUNHA, S.B (Org.). *Geomorfologia e meio ambiente*. 5ª ed. Rio de Janeiro: Bertrand Brasil, 2004. p. 59–122.
- PRUSKI, F. F. Fatores que interferem na erosão hídrica do solo. In: PRUSKI, F. F. *Conservação de água e solo: práticas mecânicas para o controle da erosão hídrica*. 2ª ed. Viçosa: editora UFV, 2009. p. 40-73.
- Ranieri S. B. L; Sparovek G.; Souza M. P; Dourado Neto D. Aplicação de Índice Comparativo na Avaliação do Risco de degradação das Terras. *Revista Brasileira de Ciência do Solo*, v. 22, n. 4, 751-760, 1998.
- Ribeiro Filho, J. C.; Santos, J. C. N; Araújo Neto, J. R.; Lemos Filho, L. C. A. Estimativa das erosividades anuais e mapeamento para o Estado do Ceará. *Revista Geonorte*. v.8, n.30, 01-15, 2017.
- ROSS, J. L. S. Geomorfologia aplicada aos EIAs-RIMA. In: GUERRA, A. J. T.; CUNHA, S. B. (Org.). *Geomorfologia e meio ambiente*. 5ª ed. Rio de Janeiro: Bertrand Brasil, 2004. p. 291 - 335.
- SALOMÃO, F.X.T. Controle e prevenção dos processos erosivos. In: GUERRA, A. J. T.; SILVA, A. S.; BOTELHO, R. G. M. (Org.). *Erosão e conservação dos solos*. 10ª ed. Rio de Janeiro: Bertrand Brasil, 2015. p. 229 - 267.
- Santa'anna Neto, J.L. A erosividade da chuva no Estado de São Paulo. *Revista do Departamento de Geografia*. v.9, 35-49, 1995.
- Silva, A. M.; Schulz, H. E.; Camargo, P. B. *Erosão e hidrossedimentologia em bacias hidrográficas*. São Carlos: Rima, 2003. 140p.
- Silva, I. B.; Mendes, L.M. S. Mapeamento de áreas susceptíveis à erosão laminar no Alto Curso do Rio Banabuiú-CE. *Revista Geoaraguaia*. v.9, n.2, 48-64, 2019.
- SILVA, M. V. C. *Análise Geoambiental: subsídios ao planejamento agrícola da Serra de Uruburetama – Ce*. Fortaleza, 2007. 191f. Dissertação (Mestrado Acadêmico em Geografia). Programa de Pós-Graduação em Geografia, Universidade Estadual do Ceará, Fortaleza-CE, 2007.
- Soares, A. *Geoestatística para as ciências da terra e do ambiente*. Lisboa: IST Press, 2006. 214p.
- Souza, M.J.N; Oliveira, V.P.V. Os enclaves úmidos e sub-úmidos do semi-árido do nordeste brasileiro. *Mercator - Revista de Geografia da UFC*, v. 5, n. 09, 85-102, 2006.
- TOLEDO, M. C.; OLIVEIRA, S. M. B.; MELFI, A. J. Intemperismo e formação do solo. In: TEIXEIRA, W.; TOLEDO, M. C. M; FAIRCHILD, T. R; TAIOLI, F. (Org.). *Decifrando a Terra*. 2ª ed. São Paulo: Oficina de textos, 2003. p. 139-166.

- 
- Yamamoto, J. K.; Landim, P. M. B. *Geoestatística: conceitos e aplicações*. São Paulo: Oficina de Textos, 2013. 215p.
- Wischmeier, W. H.; Johnson, C. B.; Cross, B. V. A soil erodibility nomograph for farmland and construction sites. *J. Journal of Soil and Water Conservation*, v. 26, n.5, 189-193, 1971.
- Wischmeier, W. H.; Smith, D. D. *Predicting rainfall erosion losses: a guide to conservation planning*. Agriculture handbook. Washington. D.C: US. Departamente of Agriculture, 1978. 60p.